

# FCC-ee $e^+e^-$ INJECTION AND BOOSTER RING

R. Ramjiawan\*, M. Barnes, W. Bartmann, J. Borburgh, Y. Dutheil, M. Hofer, E. Howling  
 CERN, Geneva, Switzerland  
 A. Chance, B. Dalena, CEA, Paris, France  
 P. J. Hunchak, University of Saskatchewan, Saskatoon, Canada

## Abstract

The Future Circular electron-positron Collider (FCC-ee) is a proposal for a 91.17 km collider, which would operate in four modes with energies ranging from 45.6 GeV (Z-pole) to 182.5 GeV ( $t\bar{t}$ -production). At high energies the beam lifetime could be as low as 6 minutes, requiring the beam to be continuously topped up to reach a high integrated luminosity. This top-up injection would use a separate booster ring in the same tunnel as the collider, which would accelerate the beams to the collider energy. The booster ring should achieve a lower equilibrium emittance than the collider, despite challenges such as a long damping time and no magnet-strength tapering to compensate for the impact of synchrotron radiation. For top-up injection into the collider, we consider two strategies: conventional bump injection, employing a closed orbit bump, and injection using a multipole kicker magnet. On-axis and off-axis sub-schemes will be studied for both. We compare these injection strategies on aspects including spatial constraints, machine protection, perturbation to the stored beam and hardware parameters.

Once the bunches are accumulated in the booster, they will be accelerated from 20 GeV to the collider energy. Operating across this energy range presents challenges for the booster, for example, achieving the necessary field quality and reproducibility between cycles at the lowest energies.

The booster ring could either be stacked vertically above the collider ring or side-by-side. Regardless of the positioning of the booster ring, injection into the collider ring must be in the horizontal plane because of the much smaller vertical emittance.

To prevent longitudinal instability of the colliding beams, the charge balance between the electron and positron beams should be kept within 3-5% of each other. This would require alternating electron and positron top-up and an injector chain which could provide bunch-to-bunch charge variations from 0-100% of the nominal value.

Table 1: FCC-ee parameters (CDR [1]) for Z- and  $t\bar{t}$ -operations. The beam lifetime is given as that from Bhabha scattering/beamstrahlung.

Parameter	Unit	Z	$t\bar{t}$
Beam energy	GeV	45.6	182.5
Beam lifetime	min	68/>200	39/18
Beam current	mA	1390	5.4
# bunches/beam		16 640	48
Magnetic rigidity	Tm	152.1	608.7
Emittance ( $x/y$ )	nm/pm	0.27/1.0	1.46/2.9
Energy spread	%	0.132	0.192

## INTRODUCTION

### The FCC-ee

The FCC-ee [1] is a proposed, high-luminosity, circular lepton collider offering the opportunity for precision study of the Higgs and electroweak sectors. To maximise the sensitivity to new physics, it would operate in four modes, from the lowest energy Z-mode to the highest energy  $t\bar{t}$ -production threshold. The lowest and highest energy machine parameters are given in Table 1. The beam lifetime would be less than an hour for the highest energies because of radiative Bhabha scattering and beamstrahlung. Therefore, to achieve a high integrated luminosity there will need to be continuous full-energy, top-up injection into the collider. During injection, the disturbance to collisions and any stoppage to data-taking in the detectors should be minimised.

Top-up injection is planned via a booster ring in the same tunnel as the collider ring. The booster would be the final stage of the FCC-ee injector chain. The beam is first accelerated within a pre-injector complex, after which it will be transferred to either a pre-booster ring, such as the CERN SPS, or a 20 GeV linac. Following this, the beam will be injected into the booster ring, where the required number of bunches will be accumulated. The booster will only hold up to 10% of the charge of the collider, so that the initial filling of the collider will need 10 injections from the booster.

### Injection into the Collider

The collider injection system is proposed to be located in the Long Straight Section (LSS) B. In these proceedings we consider two methods of top-up injection: conventional bump injection and multipole kicker injection (MKI), with off-axis and on-axis sub-schemes for each. A previous study of several top-up injection methods for lepton colliders established these as the most suitable [2]. Here, we present a comparison of the schemes with the goal of converging towards one.

By Liouville's theorem [3], the density of particles in phase-space stays constant while under conservative forces, meaning that you cannot inject particles into the phase-space of the stored bunches. Beams are instead injected with a separation from the stored beams and merge via synchrotron radiation damping. For *off-axis* injection, the bunches are injected with a transverse separation from the stored beam

\* rebecca.louise.ramjiawan@cern.ch

and perform betatron oscillations as they damp. With *on-axis* injection, bunches are injected with a momentum offset onto the off-momentum closed orbit and perform synchrotron oscillations. Consequently, for on-axis injection, there must be a non-zero dispersion at the septum to separate the on-momentum and off-momentum closed orbits.

For conventional bump injection (Fig. 1(a)), a dynamic orbit bump brings the stored beam close to the septum blade. The bump is collapsed within one revolution so that the injected beam is not lost on the septum. MKI (Fig. 1(b)) instead makes use of a multipole or non-linear kicker with a transverse field profile which would provide a kick to the injected bunch, off-axis, and a field-free region for the stored beam, on-axis.

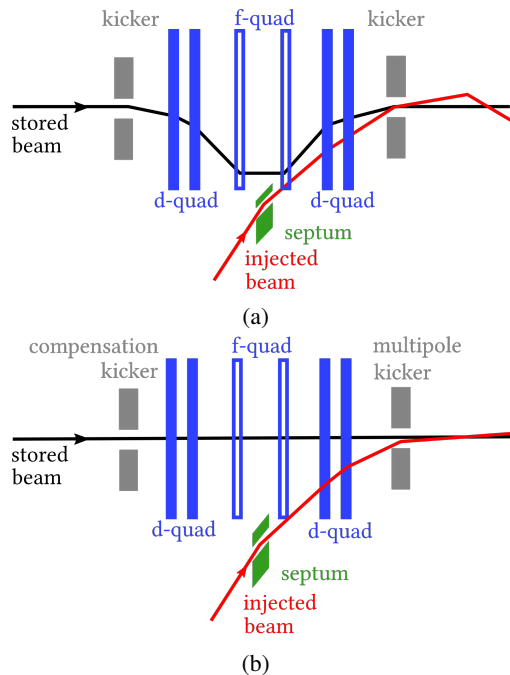


Figure 1: Schematics of the beam trajectories and beamline elements for (a) conventional bump injection and (b) multipole kicker injection [4].

In these proceedings, we consider the Z- and  $\bar{t}$ -operations because the Z-mode has the highest stored beam energy and  $\bar{t}$ -operation the highest beam rigidity. The Z-mode injection optics are presented in Fig. 2. A larger  $\beta_x$ -value at the septum means the septum width is smaller compared with the beam size, reducing its impact.

## CONVENTIONAL BUMP INJECTION

The kickers used to create the orbit bump are separated by  $\pi$ -phase-advance so as to produce a closed orbit bump with only two kickers. The orbit bump must rise and fall within one revolution to avoid beam loss on the septum. Ideally, the kicker rise and fall times should fit within the abort gap of the collider ring ( $\leq 3 \mu\text{s}$ ). To reduce the beam loss at the septum, the separation between the injected and stored beams should be  $> 5\sigma_i + S + 5\sigma_s$ , where  $\sigma$  denotes the

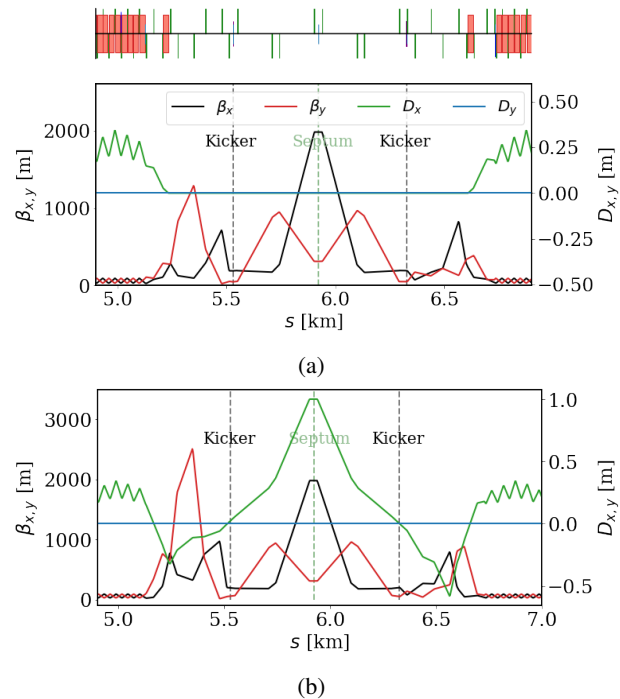


Figure 2: Injection region optics for Z-mode operation, with Twiss functions  $\beta_x$  (black),  $\beta_y$  (red) and dispersion  $D_x$  (green),  $D_y$  (blue) showing (a) off-axis injection and (b) on-axis, conventional bump injection [4]. A synoptic overview of the beamline is shown above.

r.m.s beam size, the subscripts  $i$  and  $s$  denote the injected and stored beams, and  $S$  is the septum width. The bump amplitude must be  $> 10\sigma_i + S$  to avoid losing the injected beam at the septum for subsequent revolutions.

## Optimising the Twiss Parameters

The Twiss parameters of the injected beam at the septum should be optimised to minimise the phase space needed for the injected beam [5]. To calculate the optimum parameters, simplifying assumptions were made:  $\alpha_x = 0$  and the beam angle  $x' = 0$ , for the stored and injected beams at the septum. For reference, the true value of  $\alpha_x$  for the stored beam is 0.016143. The injected beam emittance was assumed to be equal to the booster ring equilibrium emittance, 0.235 nm rad for the Z-mode. Under these conditions, the optimum  $\beta$  for the injected beam is 550 m, corresponding to a beam size of 0.35 mm.

The beam trajectories and envelopes at injection are presented in Fig. 3. This configuration was achieved with kicker deflections of  $12.5 \mu\text{rad}$  and a septum deflection of  $100 \mu\text{rad}$ . If we consider  $5\sigma$  envelopes for both beams this would allow for a 3 mm septum for Z-mode operation. For the other operation modes, depending on the injection-region optics and the emittances of the injected and stored beams, conventional bump injection may necessitate a very thin septum such as an electrostatic wire septum [6]. With a wire septum, we could achieve blade widths of the order of 100s of microns. Tracking studies are ongoing to estimate the

injection efficiency in order to compare the performance with an electrostatic versus magnetic septum.

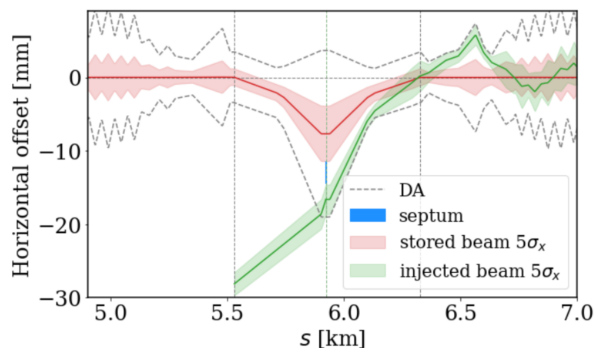


Figure 3: Injected and stored beam envelopes for off-axis conventional bump injection with optimised Twiss parameters. The  $15\sigma$  dynamic aperture (DA) is indicated with a grey dashed line.

The hardware specifications at the  $\bar{t}\bar{t}$ -threshold will be the most challenging, with a beam rigidity of 608.7 Tm. With a 182.5 GeV beam, a stripline kicker could meet the requirements for  $12.5\ \mu\text{rad}$  deflection, corresponding to an integrated electric field of 1.14 MV. For a  $50\ \Omega$  stripline kicker, with a magnetic length of 3 m and a plate separation of 20 mm, this would require a potential difference of  $\pm 3.75\ \text{kV}$ . If the two kickers were powered in series the ripples or jitter in the power supply would, ideally, cancel because of the  $\pi$ -phase-advance. However, optics errors, meaning the phase advance is not exactly  $\pi$ , or manufacturing and cabling differences between the two kickers would lead to leakage of the orbit bump. If this were the case, additional kickers could be needed to close the bump.

The kicker pulse length should cover the injection of the full booster ring, with a pulse flat-top  $>304\ \mu\text{s}$ . The repetition rate for these kickers is determined by the booster cycle-time, which is 50.95 s for the Z-mode and 5.6 s for  $\bar{t}\bar{t}$ -operation. The repetition rate for these kickers would be 0.01-0.09 Hz, taking into account the alternating electron and positron injection.

### Electrostatic Wire Septa

An electrostatic wire septum comprises many contiguous wires under tension, forming a plane separating high-field and field-free regions. In reality, in the field-free regions there is still a low field, called the leakage field. In lepton machines, these septa have an increased risk sparking caused by incident synchrotron radiation (SR). Sparking risks damage to the septum and also to the machine, if not safeguarded against. To establish whether these septa would be suitable for the FCC-ee top-up injection, there will be studies into the effect of X-rays on electrostatic septa sparking rates as a function of voltage.

Here we consider a septum deflection angle of  $100\ \mu\text{rad}$  which could be achieved with two 3-m-long modules. We assume an effective septum width of  $300\ \mu\text{m}$ . At 182.5 GeV,

the electric field strength would be 2.9 MV/m. The wire septum could be preceded by a thicker magnetic septum to reduce the deflection needed. The alignment of the beam with the wire septum is critical and would need a dedicated alignment system. Accident and failure scenarios must be considered and machine protection strategies developed to prevent the beam from impacting the septum.

### On-axis Injection

For on-axis injection, the beam is injected with a momentum offset onto the off-momentum closed orbit; this scheme is presented in Fig. 4. The dispersion needed to separate the on- and off-momentum closed orbits leads to larger beam sizes at the septum, thus requiring a larger bump height (17.1 mm), corresponding to a kicker deflection of  $27\ \mu\text{rad}$ . The momentum offset for the injected bunch,  $\delta = -1.9\%$ , is selected such that the separation between stored and injected beams,  $|D_x\delta|$ , is at least  $5\sigma_i + S + 5\sigma_s$ .

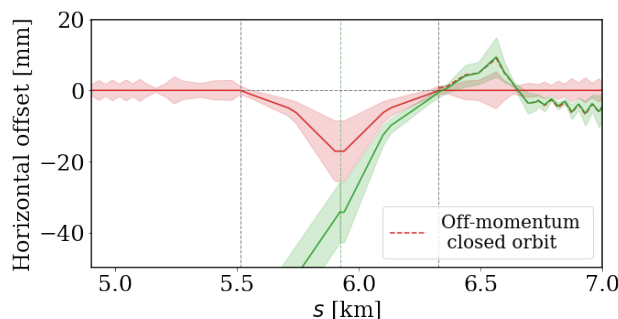


Figure 4: Beam envelopes for on-axis conventional bump injection. The beam is injected with a -1.9% momentum offset. The kicker and septum locations are denoted with dotted lines [4].

## MULTIPOLE KICKER INJECTION

The ideal multipole kicker would have zero field for the entire stored beam and a constant field for the injected beam, i.e. a step function. The design for the MKI kicker should minimise disturbance to the trajectory and distribution of the stored beam and, consequently, may offer a less disruptive injection method with a lower impact on the luminosity. A proposal for a multipole kicker design is described in [2], based on two opposing, similarly powered, C-shaped dipoles. A ‘compensation’ kicker placed  $\pi$ -phase upstream of the MKI kicker (Fig. 1) would compensate the kicker’s perturbation of the stored beam distribution and mitigate emittance blow-up. Beam distributions with and without the compensation kicker are shown in Fig. 5, highlighting its importance.

The minimum separation of the injected and stored beams at the septum ( $> 5\sigma_i + S + 15\sigma_s$ ) is larger than for conventional bump injection. The beam is injected with a  $10\sigma_x$ -offset at the kicker and the septum must remain clear of the resulting betatron oscillations. A proposal for an off-axis

Content from this work may be used under the terms of the CC-BY-4.0 licence (© 2022). Any distribution of this work must maintain attribution to the author(s), title of the work, publisher, and DOI

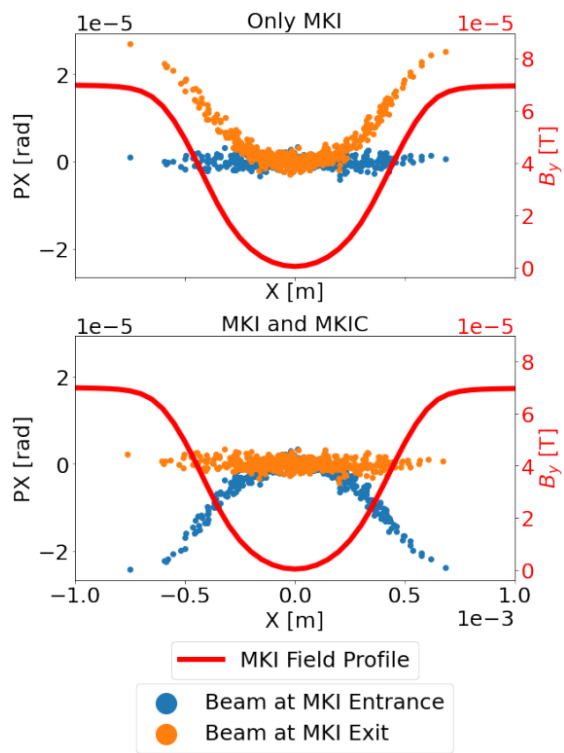


Figure 5: Tracked distributions for the stored beam at the MKI kicker entrance and exit (top) *without* a compensation kicker and (bottom) *with* a compensation kicker [7]. The MKI field profile is overlaid for comparison.

MKI injection scheme is shown in Fig. 6, with kicker deflections of 29  $\mu\text{rad}$  and a septum deflection of 100  $\mu\text{rad}$ . For MKI, a magnetic septum with a blade width of a few millimetres would be sufficient, here we assume 3 mm. The septum should have a deflecting-field-region gap-width of  $>8$  mm.

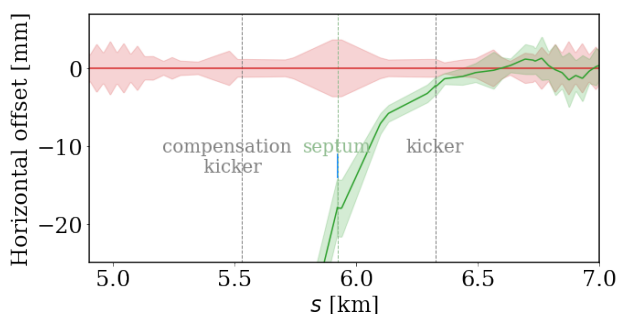


Figure 6: Beam envelopes for off-axis, multipole kicker injection [4].

### Machine Protection

For all operation modes, machine protection strategies are crucial to mitigate the risk of damage to the machine. For Z-operation, there would be 20.6 MJ of stored energy per beam. The most suitable protection methods depend on the time-scales of the failure modes. The machine could

be safeguarded against slower failures, e.g. changes in the septum field, with an active system, whereby the beam is dumped if the septum current varies by more than a few per mille. If there is a fault in the septum power supply, the magnetic field,  $B$ , will decay as  $\Delta B/B = 1 - e^{-t/\tau}$ , with the magnet decay constant,  $\tau$ . A 0.2% change in the septum would mean a 0.3 mm offset of the injected beam at the multipole kicker and, consequently,  $< 1\%$  difference in the deflection angle. If we can tolerate up to a 0.2% change in the septum, and we assume for example  $\tau = 1$  s, we would need to abort the beam in less than 7 turns (2.1 ms).

Kicker failure, either failure to fire or erratic firing, would occur on a very short timescale and, therefore, would require passive protection such as an absorber. The absorber should be placed around  $\frac{\pi}{2}$ -phase-advance from the kicker so as to be furthest from the stored beam. An example scenario for MKI where the kicker fails to fire is shown in Fig. 7; the absorber would be placed at 6.6 km.

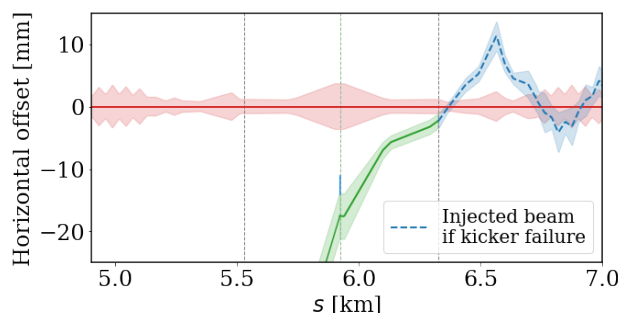


Figure 7: The injected beam trajectory if the MKI injection kicker fails to fire [4].

With conventional bump injection, the beam risks impacting the septum if the orbit bump height increases, either because of beam trajectory or kicker error, or if the beam size at the septum increases. Therefore, a mask will be needed upstream to protect the septum. Another important scenario to consider is the failure of dipoles in the transfer line from the booster to the collider. If unprotected this could lead to damage to the septum or the collider ring itself.

## BOOSTER RING

The FCC-ee booster ring will accumulate beams from either a pre-booster ring or linac and accelerate them to collider energy, ready for top-up injection. The booster ring will follow the trajectory of the collider [8], except at the interaction points (IPs) where there will be a ‘bypass’ for the booster so as to minimise synchrotron radiation to the experiments and allow for the collider IP crossing angles (Fig. 8). Injection into the booster is foreseen at site PB (Fig. 9) with the RF sections at PH and PL [9]. At site PL, 11.4 m, 400 MHz cryomodules would be arranged depending on the booster extraction energy. At PH, there would be 7.5 m, 800 MHz cryomodules only for  $\bar{t}\bar{t}$ -operation. It may instead be possible to use 800 MHz RF for all operations modes [10].

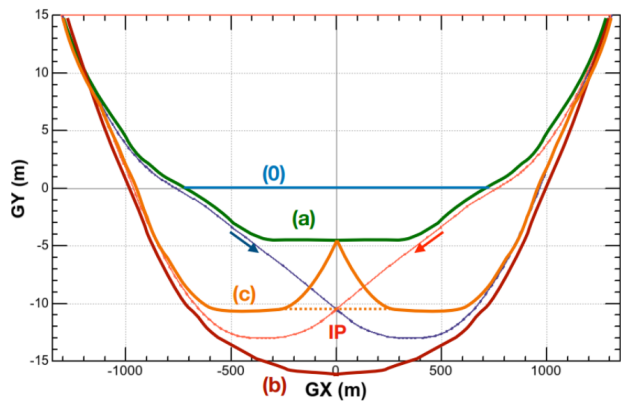


Figure 8: Options for the booster bypass regions around the collider IPs [9]. The collider-beam trajectories (thin red and blue lines) are indicated with arrows.

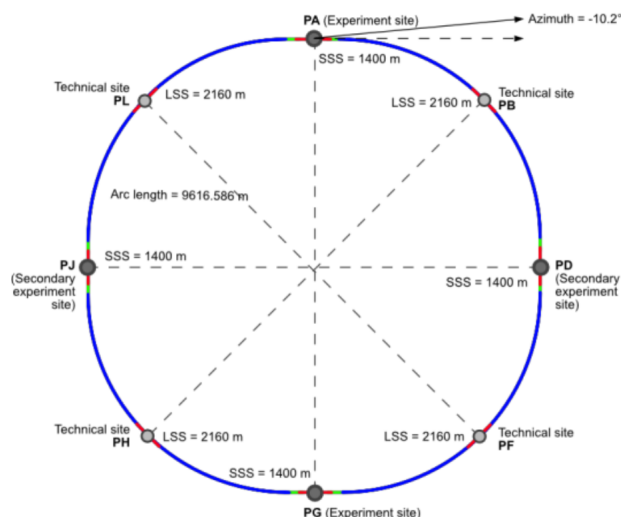


Figure 9: Booster layout indicating Long Straight Sections (LSS) and Short Straight Sections (SSS) [9].

### Injection and Extraction Systems

The booster injection system could be located in the 2160 m LSS PB. If the booster is preceded by a 20 GeV linac then two-bunch pulses would be injected at 200 Hz. These would be injected into the booster between existing stored bunches and, therefore, the injection scheme must be designed so as not to disturb the stored beam. The spacing between stored bunches is insufficient to allow an injection kicker to rise and fall, eliminating the option for on-axis, single-kicker injection. In this case, off-axis conventional bump injection would be suitable [11], either in the horizontal or vertical plane. In these proceedings, we address only horizontal injection.

Proposed injection-region optics are presented in Fig. 10. These optics have a high  $\beta_x$ -value at the septum (302 m) to minimise the kicker deflections and to minimise the impact of the septum blade. The magnet apertures in the injection region were increased to  $\pm 40$  mm to accommodate the bump injection scheme. The new optics had a maximum pole-

tip field strength of 0.73 T at the highest booster energy, 182.5 GeV [11].

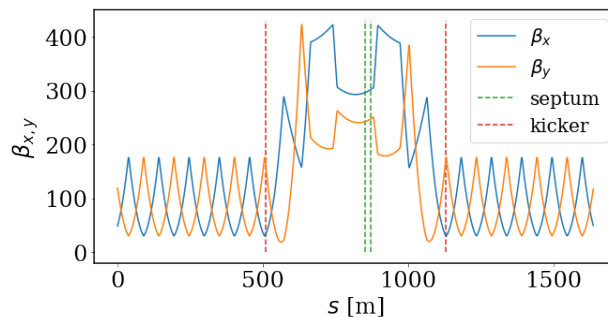


Figure 10: Booster injection-region  $\beta$ -functions.

This injection scheme uses two kickers, each providing deflections of 125  $\mu$ rad; either magnetic or stripline kicker technology would be suitable. The trajectories and envelopes of the injected and stored beams are shown in Fig. 11(a). First, a magnetic septum, with a blade width of 10 mm, provides a deflection to the injected beam of 3 mrad (integrated B-field of 2 mT m) [11]. This is succeeded by an electrostatic septum, with a blade width of 1 mm, which then deflects the beam by 0.5 mrad (integrated E-field of 3.33 MV) [11]. Just like for the collider injection, the injected beam Twiss parameters at the septum will be optimised to improve the injection efficiency.

A preliminary proposal for the extraction system is presented in Fig. 11(b). This scheme incorporates ten kickers, each providing a deflection of 43  $\mu$ rad, so that in the case one or two kickers fail the beam can still be safely extracted. A defocusing quadrupole after the kickers magnifies this deflection and, finally, two magnetic septa fully extract the beam. The septa, with blade widths of 10 mm, each provide a deflection of 4 mrad.

### Equilibrium Emittance

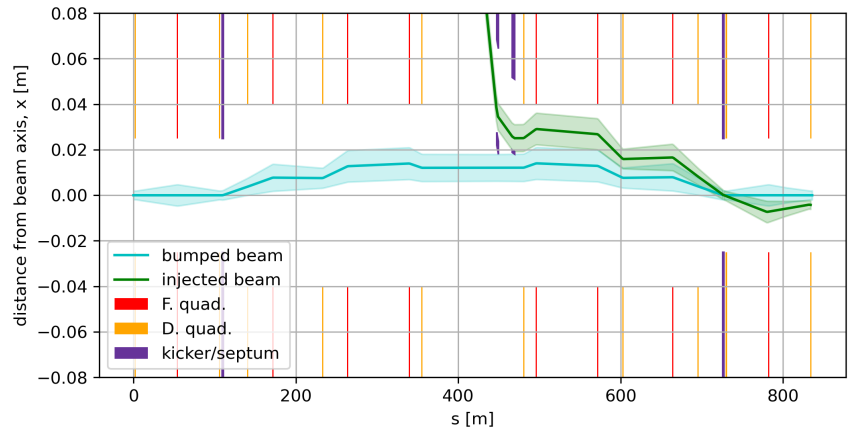
The normalized emittance of the beam injected into the booster is expected to be 50  $\mu$ m with an energy spread of 0.1%. The bunch spacing will be 15-100 ns. At the Z-pole energy for the 4IP lattice, the beam lifetime would be 1090 s so that there should be top-up injection, for each specie, every 31.61 s. This restricts the accumulation and ramp time in the booster to 24 s and 1.2 s, respectively.

Due to intra-beam scattering (IBS), the equilibrium emittance would not be reached during accumulation at 20 GeV [12]. The damping time is characterised by the second synchrotron radiation integral,  $I_2$ ,

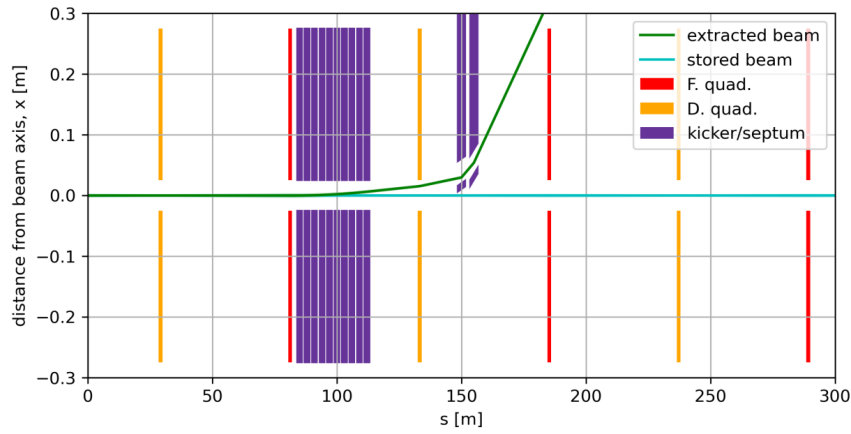
$$I_2 = \oint \frac{1}{\rho^2} ds, \quad (1)$$

with bending radius,  $\rho$ , and distance along the reference trajectory,  $s$ . The  $I_2$  of the booster ring is too small to reach the equilibrium emittance within the 1.2 s ramp time and methods to increase it were considered.

Content from this work may be used under the terms of the CC-BY-4.0 licence (© 2022). Any distribution of this work must maintain attribution to the author(s), title of the work, publisher, and DOI



(a)



(b)

Figure 11: (a) Injected and stored beam envelopes for off-axis conventional bump injection into the booster ring. Two kickers form a closed orbit bump and two septa deflect the injected beam [11]. (b) Extracted and stored beam envelopes, with an extraction system comprising ten kickers and two magnetic septa [11]. Focusing and defocusing quadrupoles are shown in red and yellow, respectively.

For the Z-mode, adding 2 s once at extraction energy would mean the collider emittance could be reached without needing to change the optics; this is demonstrated in Fig. 12. The drawback, however, would be an increase in the booster cycle-time. Alternatively, the addition of normal-conducting damping wigglers in the RF straight sections would reduce the damping time to order 0.1 s, although, at the expense of an increased equilibrium emittance [13]. These wigglers would be switched off during the energy ramp. Another option is to have an electron damping ring, which would help to meet vertical emittance targets [9].

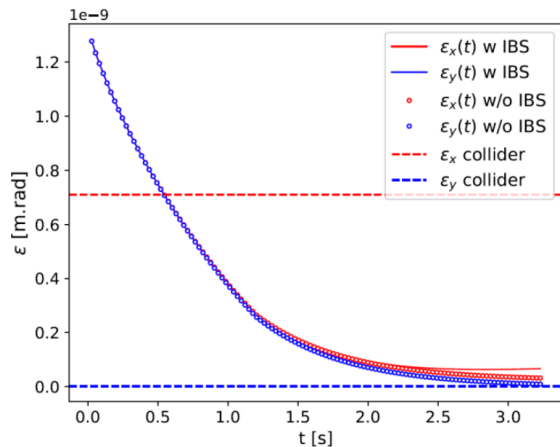


Figure 12: Emittance ( $\epsilon_{x,y}$ ) evolution in the booster ring during the ramp plus an additional 2 s at extraction energy [9], both with and without IBS, compared with the collider emittance.

Different booster optics were compared, including optics with phase advances  $\phi_{x,y} = 90^\circ/90^\circ$  or  $\phi_{x,y} = 60^\circ/60^\circ$  per FODO cell. Having the same phase advance in the horizontal and vertical planes is favourable for the chromaticity correction scheme [13]. To prevent the decrease of luminosity during top-up injection, the equilibrium emittance of the booster must be less than that of the collider ring. The equilibrium emittances for the two optics are given in Table 2, showing that only the  $90^\circ/90^\circ$  lattice is suitable for H- and  $\bar{t}$ -operation. To minimise IBS for the Z- and W-modes, the  $60^\circ/60^\circ$  lattice is preferred.

### Dynamic Aperture

For robust and efficient conventional bump injection, the dynamic aperture (DA) should be at least  $15\sigma_s$ . The booster DA at injection was estimated using MAD-X Thin-Lens tracking over 4500 turns. Alignment and multipole errors were included, as well as radiation damping and quantum excitation. The results for the  $60^\circ/60^\circ$  optics are shown in Fig. 13. The DA for the  $60^\circ/60^\circ$  optics is higher than  $20\sigma$  up to a  $\pm 0.5\%$  momentum offset, both horizontally and vertically, allowing for injection in either plane. For the  $90^\circ/90^\circ$  optics, the horizontal on-momentum DA is approximately  $15\sigma$ ; this will be optimised to increase the beam lifetime. Although, in these proceedings we have focused on horizon-

Table 2: Equilibrium emittances (r.m.s) for the booster and collider rings. Two different phase advances for the booster arc FODO cells are compared.

Beam Energy [GeV]	Equilibrium Emittance [nm rad]		
	Booster		Collider
$\phi_{x/y}$	$60^\circ/60^\circ$	$90^\circ/90^\circ$	
45.6 (Z)	0.235	0.078	0.71
80.0 (W)	0.729	0.242	2.16
120.0 (H)	4.229	0.545	0.64
175 ( $\bar{t}$ )	3.540	1.172	1.49

tal injection, for the  $90^\circ/90^\circ$  optics the DA is larger in the vertical plane which could mean a better injection efficiency for vertical injection.

## CONCLUSION

In these proceedings we have considered two options for the top-up injection of the FCC-ee collider ring: conventional bump injection and multipole kicker injection. We study off-axis and on-axis sub-schemes for both.

We have presented a scheme for conventional bump injection, with optimised Twiss parameters to improve injection efficiency. Conventional bump injection, depending on the emittance and Twiss parameters of the injected beam, might require a thin electrostatic septum with blade width of order 100s microns. R&D would be needed to determine the expected rate of sparking of the septum due to synchrotron radiation in order to establish whether this could be a suitable means of injection for such a high-energy lepton machine. MKI injection does not require such a thin septum blade and a magnetic septum would be suitable. However, R&D and prototyping would be needed to demonstrate the field quality and alignment tolerances required for this method.

Injection-region optics will also be developed for W-, H- and  $\bar{t}$ -operations and for on-axis MKI injection. These studies were for the 2IP CDR lattice [1] and will be repeated for the 4IP lattice, for which the injection insertion will need to additionally incorporate a beam crossing. Here, we have described the injection of a single beam and we will now extend this scheme to include both the electron and positron beams.

As collisions will continue during injection, the beam-beam effects during injection need careful study. The injection efficiency should be calculated and compared between the injection methods, including realistic errors and misalignments. The increased background to experiments caused by injection must also be quantified. We aim to converge to a single injection method by 2023-2024, comparing schemes based on metrics including luminosity, injection efficiency, experiment background, machine protection, feasibility, reliability and cost.

## ACKNOWLEDGEMENTS

We thank M. Aiba and M. Boland for helpful discussions. This project has received funding from the European Union's Horizon 2020 research and innovation programme under grant agreement No 951754.

## REFERENCES

- [1] FCC collaboration, "FCC-ee: The lepton collider: future circular collider conceptual design report volume 2", *Eur. Phys. J. Spec. Top.*, vol. 228, no. 2, pp. 261-623, 2019. doi:10.1140/epjst/e2019-900045-4
- [2] M. Aiba, *et al.*, "Top-up injection schemes for future circular lepton collider", *Nucl. Instrum. Methods Phys. Res. Sect. A*, vol. 880, pp. 98-106, 2018. doi:10.1016/j.nima.2017.10.075
- [3] R. L. Mills and A. M. Sessler, "Liouville's theorem and phase-space cooling", Lawrence Berkeley Lab., Berkeley, CA, USA, Rep. LBL-34667, 1993.
- [4] R. Ramjiawan, M. Aiba, W. Bartmann, Y. Duthel, M. Hofer, and P. J. Hunchak, "Concepts and considerations for FCC-ee top-up injection strategies", in *Proc. IPAC'22*, Bangkok, Thailand, Jun. 2022, pp. 2106-2109. doi:10.18429/JACoW-IPAC2022-WEPOTK025
- [5] R. P. Fliller III, "Optimal Twiss parameters for injected beam for top off injection", Brookhaven National Lab., Upton, NY, USA, Rep. Nos. NSLSII-ASD-TN-059 and BNL-211068-2019-TECH, Jul. 2018. doi:/10.2172/1504883
- [6] M.J. Barnes, J. Borburgh, B. Goddard, and M. Hourican, "Injection and extraction magnets: septa", *CERN Accelerator School: Specialised Course on magnets (Report)*, CERN, Geneva, Switzerland, Rep. CERN-2010-004, pp. 167-184, 2010.
- [7] P. Hunchak *et al.*, "Studies on Top-Up Injection Into the FCC-ee Collider Ring", in *Proc. IPAC'22*, Bangkok, Thailand, Jun. 2022, pp. 1699-1702. doi:10.18429/JACoW-IPAC2022-WEPOST011
- [8] B. Härer, B. J. Holzer, Y. Papaphilippou, and T. Tydecks, "Status of the FCC-ee top-up booster synchrotron", in *Proc. IPAC'18*, Vancouver, BC, Canada, Apr.-May 2018, pp. 250-252. doi:10.18429/JACoW-IPAC2018-MOPMF059
- [9] B. Dalena, "FCC-ee Booster Design", presented at ICHEP'22, Bologna, Italy, Jun. 2022, <https://agenda.infn.it/event/28874/contributions/169171/>
- [10] F. Peauger, "Baseline & cavity options for FCC-ee", presented at FCC Week 2022, Sorbonne Université, Paris, France, May-Jun. 2022, <https://indico.cern.ch/event/1064327/contributions/4888581/>
- [11] E. Howling, "Design studies towards the FCC-ee booster ring injection and extraction", CERN, Geneva, Switzerland, Rep. CERN-STUDENTS-Note-2022-146, 2022, <http://cds.cern.ch/record/2826991>
- [12] A. Chance, "Status of the high-energy booster", presented at FCC Week 2022, Sorbonne Université, Paris, France, May-Jun. 2022, <https://indico.cern.ch/event/1064327/contributions/4893280/>

Content from this work may be used under the terms of the CC-BY-4.0 licence (© 2022). Any distribution of this work must maintain attribution to the author(s), title of the work, publisher, and DOI

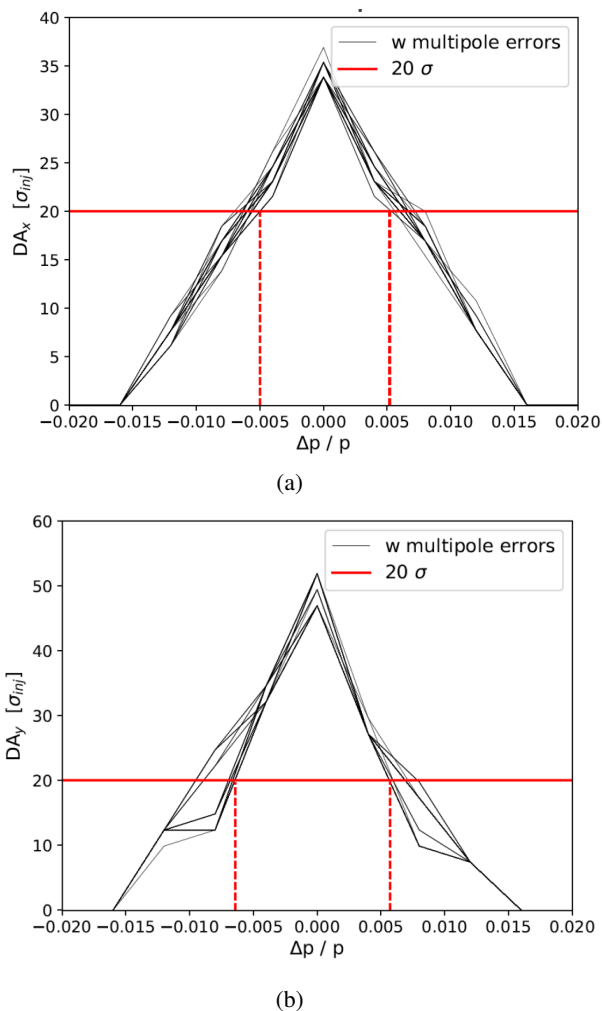


Figure 13: DA at injection for 60°/60° optics in the (a) horizontal and (b) vertical planes [9]. The grey lines show different random seeds tracked using MAD-X Thin-Lens tracking over 4500 turns.

We have given an overview of the current status of the FCC-ee booster, which will accumulate and accelerate the beams for full-energy injection into the collider. We have presented a proposal for the FCC-ee injection and extraction schemes, considering briefly the kicker and septa requirements for both. To maximise the integrated luminosity, the booster equilibrium emittance must be less than that of the collider. For the Z- and W- modes, a horizontal/vertical phase advance per FODO cell of 60°/60° was selected to reduce IBS, whereas, for the H- and  $\bar{t}$ -modes, 90°/90° phase advance was chosen to minimise the equilibrium emittance. For the booster injection, we propose a conventional bump injection scheme, which would require at least a 15σ dynamic aperture. For the 60°/60° lattice, the dynamic aperture exceeded 20σ even up to a ±0.5% momentum offset. The 90°/90° lattice has sufficient DA in the vertical plane but will need optimisation to increase the horizontal DA.



[13] B. Härer and T. Tydecks, “Lattice design and dynamic aperture studies for the FCC-ee top-up booster synchrotron”,

*arXiv preprint arXiv:2111.14462*. doi:10.48550/arXiv.2111.14462